

## The influence of curvature on membrane domains

Jeremy Pencer · Andrew Jackson · Norbert Kučerka ·  
Mu-Ping Nieh · John Katsaras

Received: 26 September 2007 / Revised: 26 February 2008 / Accepted: 7 March 2008 / Published online: 28 March 2008  
© EBSA 2008

**Abstract** An interdependence between local curvature and domain formation has been observed in both cell and model membranes. An implication of this observation is that domain formation in model membranes may be modulated by membrane curvature. In this paper, small-angle neutron scattering (SANS) is used to examine the influence of membrane curvature (i.e., vesicle size) on the formation of membrane domains. It is found that, although vesicle size and polydispersity are not significantly altered by the formation of membrane domains, the area fraction occupied by domains depends on the overall vesicle size. In particular, increasing membrane curvature (i.e., decreasing

vesicle size) results in increased area fractions of membrane domains.

### Introduction

Localized changes to membrane curvature in cells (i.e., budding and fusion) are essential for inter- and intracellular communication (McMahon and Gallop 2005). Such changes, which have been observed to drive lateral organization in model systems (Roux et al. 2005), may also lead to lateral heterogeneities in cell membranes (van Meer and Vaz 2005). In cell membranes, curvature and lateral organization are often modulated by membrane-associated proteins, commonly referred to as “coat proteins” (McMahon and Gallop 2005). However, as has been demonstrated using model systems, mechanical deformation can also drive the

---

Advanced neutron scattering and complementary techniques to study biological systems. Contributions from the meetings, “Neutrons in Biology”, STFC Rutherford Appleton Laboratory, Didcot, UK, 11–13 July and “Proteins At Work 2007”, Perugia, Italy, 28–30 May 2007.

---

J. Pencer · N. Kučerka (✉) · M.-P. Nieh · J. Katsaras  
National Research Council, Canadian Neutron Beam Centre,  
Chalk River Laboratories, Chalk River, ON K0J1J0, Canada  
e-mail: Norbert.Kucerka@nrc.gc.ca

A. Jackson (✉)  
Department of Materials Science and Engineering,  
University of Maryland, College Park, MD 20742, USA  
e-mail: ajj@nist.gov

A. Jackson  
NIST Center for Neutron Research,  
100 Bureau Drive, Bldg. 235, Stop 6102,  
Gaithersburg, MD 20899, USA

N. Kučerka  
Department of Physical Chemistry of Drugs,  
Faculty of Pharmacy, Comenius University,  
832 32 Bratislava, Slovakia

J. Katsaras  
Guelph–Waterloo Physics Institute and Biophysics  
Interdepartmental Group, University of Guelph,  
Guelph, ON N1G 2W1, Canada

J. Katsaras  
Department of Physics, Brock University,  
500 Glenridge Avenue, St Catharines, ON L2S 3A1, Canada

#### Present Address:

J. Pencer  
Atomic Energy of Canada, Ltd., Building 145, Station 68,  
Chalk River Laboratories, Chalk River, ON, Canada

formation or coalescence of domains (Roux et al. 2005). Likewise, membrane lateral heterogeneities in model systems have been observed to produce local variations in membrane curvature (Baumgart et al. 2003; Bacia et al. 2005).

Interest in the potential influence of curvature on membrane behavior is by no means new. There have been, for example, numerous studies on single component model membranes to assess the influence of curvature on both thermodynamic properties and membrane asymmetry (Marsh et al. 1977; van Dijk et al. 1978; Gruenewald et al. 1979; Eigenberg and Chan 1980; Takemoto et al. 1981; Boni et al. 1993; Nagano et al. 1995; Kučerka et al. 2007). Meanwhile, similar studies of multicomponent membranes have addressed questions related to lipid miscibility (Nordlund et al. 1981; Brumm et al. 1996). Results of these studies show that increases in membrane curvature (i.e. decreases in vesicle size) result in a shifting and broadening of the gel–fluid phase transition of single component vesicles, while influencing the miscibility and bilayer asymmetry in mixed lipid systems.

Previously, we demonstrated that small-angle neutron scattering (SANS) was an effective technique for the detection and characterization of membrane domains in unilamellar vesicles (ULV) (Pencer et al. 2005). It was observed that domain formation in sub-micron-sized ULV occurred over a similar composition and temperature range as in micron-sized giant unilamellar vesicles (GUV), but the data could not be interpreted simply either in terms of single or multiple domains (Pencer et al. 2005). More recent SANS studies on binary mixtures also demonstrated domain formation, but failed to produce results consistent with known phase diagrams (Anghel et al. 2007). Such inconsistencies may indicate a possible influence of membrane curvature on lipid miscibility in ULV, since lipid phase diagrams for binary and ternary lipid mixtures have been constructed from data using either multilamellar vesicles (MLV) (van Dijk et al. 1977) or GUV (Veatch et al. 2004), both having significantly lower curvatures than ULV.

The primary purpose of this study was to demonstrate the applicability of the recently developed state of the art approach in studying the lateral membrane domains and to reconcile the apparent discrepancies arising from the different studies. We assessed the possible influence of membrane curvature (vesicle size) on the relative size (area fraction) of membrane domains. A ternary mixture of DOPC, DPPC and cholesterol was examined, since this mixture has been well characterized (e.g. Veatch et al. 2004), and is expected to produce a single circular domain per vesicle (Yanagisawa et al. 2007). The temperature of 10°C was chosen to ensure the coexistence of a liquid disordered phase and liquid ordered or gel phase in all

samples studied (different deuteration and vesicle sizes). Measurements were performed using two contrast conditions allowing for a separate assessment of the vesicle form factor and contribution to scattering from lateral heterogeneities (e.g. Pencer et al. 2006). We find that vesicle size and polydispersity are not significantly perturbed by the formation of membrane domains, but that the area fraction occupied by domains depends on the overall vesicle size.

## Materials and methods

### Materials

1,2-dipalmitoyl-D62-sn-glycero-3-phosphocholine (dDPPC), 1,2-dipalmitoyl-sn-glycero-3-phosphocholine (DPPC), 1,2-dioleoyl-sn-glycero-3-phosphocholine (DOPC), Na-1,2-dipalmitoyl-sn-glycero-3-phosphatidylserine (DPPS), Na-1,2-dioleoyl-sn-glycero-3-phosphatidylserine (DOPS), and cholesterol, were purchased from Avanti Polar Lipids, Inc. (Birmingham, AL) as lyophilized powders and used without further purification. Upon arrival, the ampules containing the various lipids were stored at  $-80^{\circ}\text{C}$ . Ninety-nine percent purity  $\text{D}_2\text{O}$  was purchased from Cambridge Scientific (Andover, MA), while all other chemicals were reagent grade.

### Vesicle preparation

ULV were prepared by extrusion as described in MacDonald et al. (1991). Lipid mixtures of DPPC, DOPC and cholesterol were doped with 4 mol% phosphatidylserine (PS) in order to encourage the unilamellarity of the larger sized vesicles (Kučerka et al. 2007). Equal proportions of DPPS and DOPS were used to ensure uniform distribution of the charged lipid. In some samples, the DPPC fraction contained 70 mol% chain deuterated lipid (dDPPC). Lipids solubilized in chloroform were transferred to glass vials in appropriate proportions to produce solubilized lipid mixtures of predetermined molar ratios and the chloroform was removed under a stream of  $\text{N}_2$  followed by vacuum pumping. The molar ratio of DPPC:DPPS:DOPC:DOPS:cholesterol was 4.3:0.2:4.3:0.2:1. Lipid films were then preheated to  $60^{\circ}\text{C}$  and dispersed in either 36% (partially deuterated lipid) or 100%  $\text{D}_2\text{O}$  (fully protonated lipid), also preheated to  $60^{\circ}\text{C}$ . The lipid dispersions were then extruded using a hand-held extruder purchased from Avanti Polar Lipids (Birmingham, AL), which was preheated to  $60^{\circ}\text{C}$  prior to extrusion. Total lipid concentrations ranged from 1 to 10 mg/ml. Extrusion was used to produce ULV with nominal sizes of 50, 100, and 200 nm. The 50 nm ULV were formed by successive extrusions using three different pore diameter polycarbonate filters, and a total of

43 passes (e.g. 200-nm (9 times), 100-nm (9 times) and 50-nm (25 times)). The 100 and 200 nm vesicles were extruded using a total of 34 (e.g. 200-nm (9 times), 100-nm (25 times)) and 25 (e.g. 200-nm (25 times)) passes, respectively.

Small-angle neutron scattering

SANS measurements were performed using the 30 m NG3 SANS (Glinka et al. 1998) and BT5 USANS (Barker et al. 2005) instruments located at NIST (Gaithersburg, MD). On the NG3 instrument, measurements were performed using three sample-detector distances (SDD), 12 m, 5 and 1 m. 6 Å wavelength ( $\lambda$ ) neutrons were used at 12 SDD and 5 m SDD and 5 Å neutrons at 1 m SDD. The  $\delta\lambda/\lambda$  was 15% for both wavelengths. The combined SANS instrument configurations gave a total  $q$  range of  $0.004 < q < 0.4 \text{ \AA}^{-1}$ , where  $q = 4\pi\sin(\theta/2)/\lambda$ ,  $\theta$  is the scattering angle, and  $\lambda$  is the neutron wavelength. The BT-5 USANS instrument uses 2.38 Å neutrons and routinely allows access to a  $q$  range of  $5 \times 10^{-5} < q < 5 \times 10^{-3} \text{ \AA}^{-1}$ . As a result of the vertical line beam profile of the instrument, with a corresponding  $\Delta Q_v$  of  $0.117 \text{ \AA}^{-1}$ , the observed beam intensity at any nominal  $Q_h$  is a convolution of a range of actual  $Q$  values. Although the observed data can either be desmeared by iterative (Lake 1967) or direct (Singh et al. 1993) methods, the preferred approach (and that taken here) is to smear the model function with the resolution function of the instrument as follows

$$\frac{d\Sigma_s}{d\Omega}(q) = \frac{1}{\Delta q_v} \int_0^{\Delta q_v} \frac{d\Sigma}{d\Omega}(\sqrt{q^2 + u^2}) du, \tag{1}$$

where  $d\Sigma_s/d\Omega(q)$  is the slit smeared scattering cross section.

SANS and USANS data were reduced and corrected for sample transmission and background using Igor Pro with routines provided by the NIST Center for Neutron Research (NCNR) (Kline 2006). SANS data were fit using routines provided by the NCNR (Kline 2006) and our own fitting routines (Anghel et al. 2007).

Scattering length density and match point determination

As discussed in Pencer et al. (2006), the optimal conditions for the detection and characterization of membrane domains are significantly different from those that are optimal for the measurement of the vesicle form factor. In this study, the vesicle form factor is obtained from scattering measurements of protonated ULV in 100% D<sub>2</sub>O, producing the maximum contrast between the membrane and the medium, while minimizing the contrast between potential membrane heterogeneities. To detect and

characterize membrane domains, ULV are prepared under conditions where the mean acyl chain scattering length density (SLD), lipid headgroup SLD, and medium SLD are all approximately equal (i.e. contrast matched conditions). Under these conditions the only observable scattering will result from the contrast between membrane domains and the medium. Note, that the isotopic labeling of bilayer components has a negligible effect on its thermodynamical properties under the particular conditions selected in this study. However, this is not the case in the vicinity of the phase transition temperature, which can be shifted by several degrees. For example, the main (gel–fluid) transition occurs at 41.7°C for protonated DPPC, while it is about 4°C lower for chain deuterated DPPC (Katsaras et al. 1997).

To obtain the described contrast matched conditions it is necessary to estimate the SLD of the lipid headgroup and acyl chain regions, which can be calculated as

$$\rho_i = b_i/V_i, \tag{2}$$

where  $\rho_i$ ,  $b_i$  and  $V_i$  are the SLD, scattering length and molecular volume of component  $i$ , respectively, and which can be calculated from known scattering lengths (Sears 1992) and component volumes (Knoll et al. 1981; Nagle and Tristram-Nagle 2000). These values are summarized in Table 1. The mean SLD of the headgroup and acyl chain regions are calculated as in Pencer et al. (2005) and Anghel et al. (2007) as

$$\rho = \frac{\sum_i n_i V_i \rho_i}{\sum_i n_i V_i}, \tag{3}$$

**Table 1** Neutron scattering lengths,  $b$ , component volumes,  $V$ , and neutron scattering length densities,  $\rho$ , for the lipids and their components used in this study

Molecule	$b$ (fm)	$V$ (Å <sup>3</sup> )	$\rho$ (Å <sup>-2</sup> )
DPPC, C <sub>40</sub> H <sub>80</sub> NO <sub>8</sub> P	27.63	1,232	$0.22 \times 10^{-6}$
Head, C <sub>10</sub> H <sub>18</sub> NO <sub>8</sub> P	60.1	326	$1.84 \times 10^{-6}$
Chains, C <sub>30</sub> H <sub>62</sub>	-32.4	891	$-0.36 \times 10^{-6}$
dDPPC, C <sub>40</sub> H <sub>18</sub> NO <sub>8</sub> PD <sub>62</sub>	672.99	1232	$5.46 \times 10^{-6}$
Head, C <sub>10</sub> H <sub>18</sub> NO <sub>8</sub> P	60.1	326	$1.84 \times 10^{-6}$
Chains, C <sub>30</sub> D <sub>62</sub>	613	891	$6.88 \times 10^{-6}$
DOPC, C <sub>44</sub> H <sub>84</sub> NO <sub>8</sub> P	39.26	1,303	$0.30 \times 10^{-6}$
Head, C <sub>10</sub> H <sub>18</sub> NO <sub>8</sub> P	60.1	337	$1.78 \times 10^{-6}$
Chains, C <sub>34</sub> H <sub>66</sub>	-13.3	981	$-0.14 \times 10^{-6}$
DPSP, C <sub>38</sub> H <sub>73</sub> NO <sub>10</sub> P	52.0	1,232	$0.42 \times 10^{-6}$
Head, C <sub>8</sub> H <sub>11</sub> NO <sub>10</sub> P	84.5	326	$2.59 \times 10^{-6}$
Chains, C <sub>30</sub> H <sub>62</sub>	-32.4	891	$-0.36 \times 10^{-6}$
DOPS, C <sub>42</sub> H <sub>77</sub> NO <sub>10</sub> P	63.6	1,303	$0.49 \times 10^{-6}$
Head, C <sub>8</sub> H <sub>11</sub> NO <sub>10</sub> P	84.5	337	$2.51 \times 10^{-6}$
Chains, C <sub>34</sub> H <sub>66</sub>	-13.3	981	$-0.14 \times 10^{-6}$
Cholesterol, C <sub>27</sub> H <sub>46</sub> O	13.25	629	$0.21 \times 10^{-6}$

where  $n_i$ ,  $V_i$ , and  $\rho_i$  are the mole fraction, component volume and SLD of molecules of type  $i$ , respectively, making up either the headgroup or acyl chain region. For a mixture of 4.3:0.2:4.3:0.2:1 DPPC:DPPS:DOPC:DOPS: cholesterol, we determine an average SLD of  $1.9 \times 10^{-6} \text{ \AA}^{-2}$  for the lipid headgroup region. In order to obtain a similar value for the SLD of the acyl chain region, a molar ratio of 0.7:0.3 dDPPC:DPPC was used, giving a molar composition of 3.3:1:0.2:4.3:0.2:1 dDPPC:DPPC:DPPS: DOPC:DOPS: cholesterol. The corresponding mean SLD is contrast matched with 36%  $\text{D}_2\text{O}$ .

## Theory

As discussed in Yanagisawa et al. (2007), for ternary mixtures of DOPC:DPPC:cholesterol, liquid domains on each vesicle are expected to coalesce into a single circular domain as long as the entrapped vesicle volume is not osmotically constrained. Since the ULV used in this study were prepared in pure water, their volumes are not osmotically constrained, and so, are expected to produce single, circular domains at equilibrium. Note, however, that the assumption of completely segregated circular domains in each vesicle is not a necessary condition for our analysis. Since ULV will undergo rotational diffusion over the course of the SANS measurements, and these measurements sample a large number of ULV, the SANS results provide an orientational and ensemble average. As such, fits to SANS data using the single circular domain approximation provide information concerning the “effective” or circular-domain-equivalent size of ULV membrane heterogeneities. The main features of this model will be discussed below, while a more detailed discussion and derivation of the heterogeneous form factor can be found in Anghel et al. (2007).

As shown in Fig. 1 the SLD of a vesicle with a circular domain is axially symmetric and can be represented by a function of two parameters in spherical coordinates, i.e.  $\rho(r, \theta)$ . We shall assume that the SLD is constant with respect to  $\theta$ , both inside and outside of the domain, and that the domain interface is sharp and bounded by the angle  $\alpha$ . We define the SLD inside the domain to be  $\rho_1(r)$  and outside to be  $\rho_2(r)$ . For convenience, we will define the total vesicle SLD,  $\rho(r, \theta)$ , as a sum of a homogeneous contribution,  $\rho_w(r)$ , and a heterogeneous contribution,  $\rho_v(r, \theta)$ ,

$$\rho(r, \theta) = \rho_w(r) + \rho_v(r, \theta), \quad (4)$$

where

$$\rho_w(r) = \rho_2(r), 0 \leq \theta \leq \pi, \quad (5)$$

$$\rho_v(r, \theta) = \rho_1(r) - \rho_2(r), 0 \leq \theta \leq \alpha. \quad (6)$$

The form factor for vesicles with single circular domains can then be calculated as (Anghel et al. 2007)

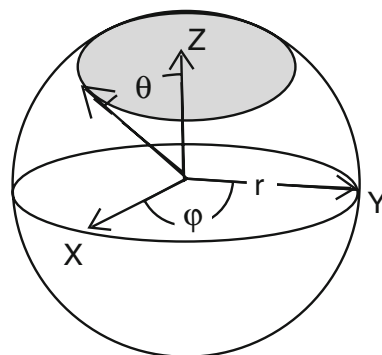


**Fig. 1** Schematic of a heterogeneous vesicle. The circle defined by the angle  $\theta$  forms the boundary of a circular domain, centered on the  $z$  axis, of a vesicle of radius  $r$

$$I(q) = \left\{ \frac{2Z_w(q, R) + Z_0(q, R)X_0(\alpha)}{q} \right\}^2 + \frac{1}{q^2} \sum_{l=1}^{\infty} (2l+1)^2 Z_l^2(q, R) X_l^2(\alpha), \quad (7)$$

where  $R$  is the vesicle radius. The homogeneous vesicle contribution,  $Z_w(q, R)$  is given by

$$Z_w(q, R) = q \int_0^{\infty} [\rho_w(r) - \rho_m] r^2 j_0(qr) dr, \quad (8)$$

where  $\rho_m$  is the SLD of the aqueous medium, and heterogeneous vesicle contributions,  $X_l(\alpha)Z_l(q, R)$ , are

$$X_0(\alpha) = 1 - \cos \alpha, \quad (9)$$

$$X_l(\alpha) = \frac{1}{l} [\cos \alpha P_l(\cos \alpha) - P_{l+1}(\cos \alpha)], \quad l \neq 0 \quad (10)$$

and

$$Z_l(q, R) = q \int_0^{\infty} \rho_v(r) j_l(qr) dr, \quad (11)$$

where the  $P_l$  and  $j_l$  are the Legendre polynomials and spherical Bessel functions of order  $l$ , respectively.

For laterally homogeneous vesicles, Eq. 7 reduces to (e.g. Pencer and Hallett 2003):

$$I(q) = \left\{ \frac{2Z_w(q, R)}{q} \right\}^2. \quad (12)$$

Note, that for the purposes of fitting experimental data, both Eqs. 7 and 12 are integrated over the vesicle size distribution (Anghel et al. 2007) and the instrumental resolution function (Glinka et al. 1998; Barker et al. 2005; Kline 2006).

## Results and discussion

### Determination of the vesicle form factor

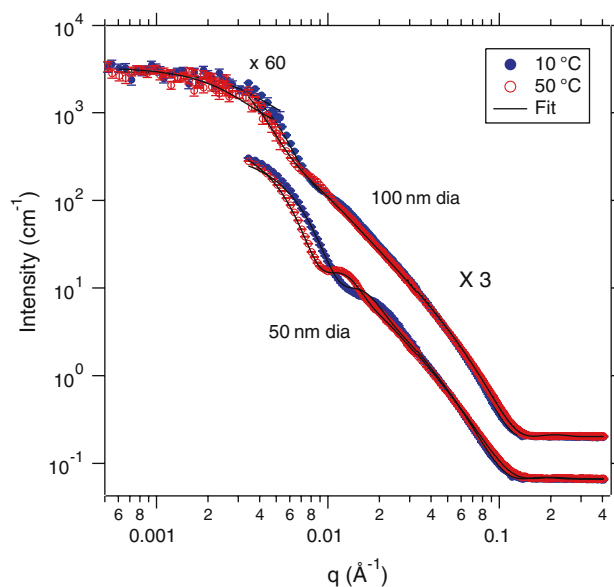
Changes in temperature, and the formation of membrane domains can influence vesicle shape and stability (e.g. Lipowsky and Dimova 2003). Furthermore, while it previously has been demonstrated that the extrusion technique generally produces ULV of well defined size and polydispersity (Macdonald et al. 1991), there are cases where preparations of large ULV can be contaminated by the presence of paucilamellar vesicles (PLV) (Schmiedel et al. 2006; Kučerka et al. 2007). To verify that the ULV used in this study were unilamellar and that their structures were not significantly perturbed by temperature changes, or the formation of domains, SANS data were collected from ULV using protonated lipid in 100% D<sub>2</sub>O. Under these contrast conditions, lipid lateral heterogeneity does not produce significant lateral variations in SLD, since all lipids present have essentially the same acyl chain SLD. Consequently, the ULV SANS data can be interpreted using the homogeneous vesicle form factor given by Eq. 12, thus obtaining the mean vesicle size, polydispersity and membrane thickness, as a function of temperature and nominal diameter.

Figure 2 shows SANS data obtained from 50 to 100 nm nominal diameter protonated ULV in 100% D<sub>2</sub>O and at 10 and 50°C. The corresponding fits to the data were obtained using Eq. 12. Fit results are summarized in Table 2. For the 200 nm diameter ULV, the data could not be successfully fit with a vesicle form factor (not shown), most likely due to contamination of the sample by pauci (PLV) or multilamellar vesicles (MLV) (Kučerka et al. 2007), although the obtained mean characteristics of the system were consistent with the results shown in Table 2. Consequently, further discussions will be restricted to results obtained for 50 and 100 nm diameter vesicles.

A temperature shift from 10 to 50°C results in an increase in the mean vesicle radius and concomitant decrease in the membrane thickness. However, the overall vesicle structure is unperturbed by temperature changes. Agreement between the fits and the experimental data for the two smaller ULV systems also confirms that the vesicles are predominantly unilamellar. The ULV size, polydispersity and thickness obtained from these fits will be used later on to facilitate the fitting of SANS data from ULV with laterally heterogeneous SLD.

### Detection and measurement of membrane domains

The primary objectives of this study are to do a qualitative comparison between the domain formation in vesicles of different size. As discussed in Pencer et al. (2006),



**Fig. 2** Colour online. Small angle neutron scattering curves from protonated ULV in 100% D<sub>2</sub>O. Curves have been shifted on the vertical scale to facilitate viewing. Measurements have been obtained at two temperatures, 10°C (solid blue symbols) and 50°C (open red symbols). The solid black lines represent fits to the data

**Table 2** Fitting results for protonated ULV in D<sub>2</sub>O

D <sub>nom</sub> (Å)	T (°C)	$\langle D \rangle$ (Å)	$\sigma/\langle D \rangle$	t (Å)
500	10	441.2 ± 3.6	0.26 ± 0.01	46.7 ± 0.3
500	50	605.2 ± 3.0	0.23 ± 0.01	41.6 ± 0.1
1000	10	621.8 ± 10.4	0.32 ± 0.01	45.3 ± 0.2
1000	50	728.4 ± 23.2	0.43 ± 0.02	40.6 ± 0.1

First column reports the nominal diameter, T refers to the temperature,  $\langle D \rangle$  is the mean vesicle diameter,  $\sigma/\langle D \rangle$  is the relative polydispersity, and t is the membrane thickness

scattering from laterally heterogeneous vesicles will have three contributions: (1) The homogeneous vesicle contribution, (2) the contribution due to the contrast between the acyl chain and headgroup regions, and (3) the contribution due to the contrast between the membrane domains. The optimal conditions for the measurement of (3) correspond to minimizing (1) and (2). Here, we achieve these optimal contrast conditions by using a mixture of DPPC and dDPPC in proportions such that the mean acyl chain SLD is equal to that of the headgroup region. By contrast matching the mean ULV SLD, using 36% D<sub>2</sub>O, we are able to suppress both (1) and (2). Note, that under these conditions the zeroth order term (corresponding to the homogeneous vesicle contribution) in Eq. 7 vanishes. Consequently, while it is possible to determine the size of a circular domain on a vesicle,  $\alpha$ , it is not possible to obtain independent values for  $\rho_1$  and  $\rho_2$ , since the scattered intensity is proportional to  $(\rho_2 - \rho_1)^2$ .

SANS data for the same sized ULV as above, but with partially deuterated lipid dispersed in 36% D<sub>2</sub>O, are shown in Fig. 3. At high temperatures we expect that the lipids will be homogeneously mixed in the ULV and will not produce a scattering signal. At low temperatures, however, we expect to see excess scattering due to lateral heterogeneities. Contrary to our expectations we observe that both vesicle sizes show a forward scattering signal at 50°C. We have observed this phenomenon previously (Pencer et al. 2005) and attributed it to imperfect contrast matching of the samples, either in matching the mean acyl chain SLD to that of the headgroups, or that of the medium to the vesicles. Fits to the high temperature data shown in Fig. 3 with the same vesicle structural parameters as obtained above (Table 2), confirm that the scattering signal corresponds to the homogeneous vesicle form factor.

More importantly, at 10°C we observe a much larger scattering signal for both ULV systems, consistent with our expectation of the formation of membrane domains. We should note that, based on our previous studies (Pencer et al. 2005) we are confident that the scattering signal is not due to trivial contributions such as, increased contrast due to the density change in the lipid bilayer concomitant with thermal expansion or contraction.

Fits to low temperature data are shown in Fig. 3 using the model for vesicles with circular domains, given by Eq. 7. According to the previously established fitting procedure (Anghel et al. 2007), we constrain the mean ULV

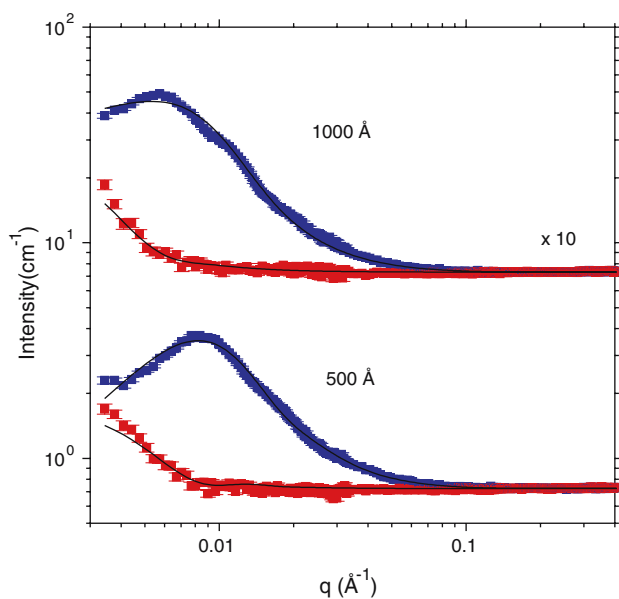


**Fig. 3** Colour online. Small angle neutron scattering curves from partially deuterated ULV in 36% D<sub>2</sub>O. Curves have been shifted on the vertical scale to facilitate viewing. Measurements have been obtained at two temperatures, 10 (blue symbols) and 50°C (red symbols). Fits to the data are shown with solid lines

**Table 3** Fitting results for partially deuterated ULV in 36% D<sub>2</sub>O measured at 10°C

$\langle D \rangle$ (Å)	$\alpha$ (rad)	$a_0$
441.2	$0.95 \pm 0.02$	$0.21 \pm 0.01$
728.4	$0.63 \pm 0.03$	$0.10 \pm 0.01$

$\langle D \rangle$  is the mean vesicle diameter,  $\alpha$  is the angle defining the domain size, and  $a_0$  gives the relative area fraction of the domain

radius, polydispersity and thickness in performing fits to the heterogeneous ULV SANS data based on the results from the protonated vesicles. As discussed, because of the diminishing contribution of the zeroth order term in Eq. 7, we are only able to determine the domain size,  $\alpha$ , and neither  $\rho_1$  and  $\rho_2$ . Fitting results for ULV systems with nominal diameters of 50 and 100 nm are summarized in Table 3. Results for the 200 nm diameter ULV are omitted as mentioned.

Interestingly, we find that the apparent relative size and area fraction of circular domains decreases as a function of increasing vesicle radius. This result is consistent with the observations of Brumm et al. (1996), who found increased demixing of lipids with increasing curvature in binary mixed lipid bilayers on spherical silica supports. Nevertheless, to the best of our knowledge, ours is the first such observation of a similar phenomenon in ternary mixtures of freely suspended bilayers.

## Conclusions

There is ongoing controversy regarding the size and stability of membrane domains in both cell and model membranes. This controversy is further complicated by the variability in sensitivity among the techniques used to detect domains, as well as the variety of model systems used in membrane domain studies. In particular, the observation of lateral heterogeneities in ULV by fluorescence resonance energy transfer (FRET), where none are observed in GUV by fluorescence microscopy (FM), has led to fundamental questions regarding the nature of membrane domains (Feigenson and Buboltz 2001). Here, we have found that membrane curvature has a significant effect on the miscibility of lipid components, in particular, that increased membrane curvature (decreased ULV size) produces increased demixing of lipids, as observed through increased relative domain area fraction. An implication of these results is that apparent inconsistencies between FRET on ULV and FM on GUV may be merely an artefact of differences in membrane curvature.

**Acknowledgments** The authors gratefully acknowledge Vini Anghel and Thalia Mills for valuable and enjoyable discussions. This work utilized facilities supported in part by the National Science

Foundation under Agreement No. DMR-0454672. We acknowledge the support of the National Institute of Standards and Technology, U.S. Department of Commerce, in providing the neutron research facilities used in this work. Certain commercial equipment, instruments, or materials (or suppliers, or software, ...) are identified in this paper to foster understanding. Such identification does not imply recommendation or endorsement by the National Institute of Standards and Technology, nor does it imply that the materials or equipment identified are necessarily the best available for the purpose.

## References

- Anghel VNP, Kučerka N, Pencser J, Katsaras J (2007) Scattering from laterally heterogeneous vesicles II: the form factor. *J Appl Cryst* 40:513–525
- Bacia K, Schwille P, Kurzchalia T (2005) Sterol structure determines the separation of phases and the curvature of the liquid-ordered phase in model membranes. *Proc Natl Acad Sci USA* 102:3272–3277
- Barker JG, Glinka CJ, Moyer JJ, Kim MH, Drews AR, Agamalian M (2005) Design and performance of a thermal-neutron double-crystal diffractometer for USANS at NIST. *J Appl Cryst* 38:1004–1011
- Baumgart T, Hess ST, Webb WW (2003) Imaging coexisting fluid domains in biomembrane models coupling curvature and line tension. *Nature* 425(2003):821–824
- Boni LT, Minchey SR, Perkins WR, Ahl PL, Slater JL, Tate MW, Gruner SM, Janoff AS (1993) Curvature dependent induction of the interdigitated gel phase in DPPC vesicles. *Biochim Biophys Acta* 1146:247–257
- Brumm T, Jørgensen K, Mouritsen OG, Bayerl T (1996) The effect of increasing membrane curvature on the phase transition and mixing behavior of a dimyristoyl-sn-glycero-3-phosphatidyl choline/distearoyl-sn-glycero-3-phosphatidyl choline lipid mixture as studied by Fourier transform infrared spectroscopy and differential scanning calorimetry. *Biophys J* 70:1373–1379
- Eigenberg KE, Chan SI (1980) The effect of surface curvature on the head-group structure and phase transition properties of phospholipid bilayer vesicles. *Biochim Biophys Acta* 599:330–335
- Feigenson GW, Buboltz JT (2001) Ternary phase diagram of dipalmitoyl-PC/dilauroyl-PC/cholesterol: nanoscopic domain formation driven by cholesterol. *Biophys J* 80:2775–2788
- Glinka CJ, Barker JG, Hammouda B, Krueger S, Moyer JJ, Orts WJ (1998) The 30 m small-angle neutron scattering instruments at the National Institute of Standards and Technology. *J Appl Cryst* 31:430–445
- Gruenewald B, Stankowski S, Blume A (1979) Curvature influence on the cooperativity and the phase transition enthalpy of lecithin vesicles. *FEBS Lett* 102:227–229
- Katsaras J, Epand RF, Epand RM (1997) Absence of chiral domains in mixtures of dipalmitoylphosphatidylcholine molecules of opposite chirality. *Phys Rev E* 55:3751–3753
- Kline SR (2006) Reduction and analysis of SANS and USANS data using IGOR Pro. *J Appl Cryst* 39:895–900
- Knoll W, Haas J, Stuhmann HB, Fuldner HH, Vogel H, Sackmann E (1981) Small-angle neutron scattering of aqueous dispersions of lipids and lipid mixtures. A contrast variation study. *J Appl Cryst* 14:191–202
- Kučerka N, Pencser J, Sachs JN, Nagle JF, Katsaras J (2007) Curvature effect on the structure of phospholipid bilayers. *Langmuir* 23:1292–1299
- Lake JA (1967) An iterative method of slit-correcting small angle X-ray data. *Acta Cryst* 23:191–194
- Lipowsky R, Dimova R (2003) Domains in membranes and vesicles. *J Phys Condens Matter* 15:S31–S45
- MacDonald RC, MacDonald RI, Menco BPhM, Takeshita K, Subbarao NK, Hu L-r (1991) Small-volume extrusion apparatus for preparation of large, unilamellar vesicles. *Biochim Biophys Acta* 1061:297–303
- Marsh D, Watts A, Knowles PF (1977) Cooperativity of the phase transition in single- and multibilayer lipid vesicles. *Biochim Biophys Acta* 465:500–514
- McMahon HT, Gallop JL (2005) Membrane curvature and mechanisms of dynamic cell membrane remodelling. *Nature* 438:590–596
- Nagano H, Nakanishi T, Yao H, Ema K (1995) Effect of vesicle size on the heat capacity anomaly at the gel to liquid-crystalline phase transition in unilamellar vesicles of dimyristoyl phosphatidylcholine. *Phys Rev E* 52:4244–4250
- Nagle JF, Tristram-Nagle S (2000) Structure of lipid bilayers. *Biochim Biophys Acta* 1469:159–195
- Nordlund JR, Schmidt CF, Dicken SN, Thompson TE (1981) Transbilayer distribution of phosphatidylethanolamine in large and small unilamellar vesicles. *Biochemistry* 20:3237–3241
- Pencser J, Hallett FR (2003) Effects of vesicle size and shape on static and dynamic light scattering measurements. *Langmuir* 19:7488–7497
- Pencser J, Mills T, Anghel VNP, Krueger S, Epand RM, Katsaras J (2005) Detection of submicron-sized raft-like domains in membranes by small-angle neutron scattering. *Eur Phys J E* 18:447–458
- Pencser J, Anghel VNP, Kučerka N, Katsaras J (2006) Scattering from laterally heterogeneous vesicles I: model independent analysis. *J Appl Cryst* 39:791–796
- Roux A, Cuvelier D, Nassoy P, Prost J, Bassereau P, Goud B (2005) Role of curvature and phase transition in lipid sorting and fission of membrane tubules. *EMBO J* 24:1537–1545
- Schmiedel H, Almásy L, Klose G (2006) Multilamellarity, structure and hydration of extruded POPC vesicles by SANS. *Eur Biophys J* 35:181–189
- Sears V (1992) Neutron scattering lengths and cross sections. *Neutron News* 3:26–37
- Singh MA, Gosh SS, Shannon RF (1993) A direct method of beam-height correction in small-angle X-ray-scattering. *J Appl Cryst* 26:787–794
- Takemoto H, Inoue S, Yasunaga T, Sukigara M, Toyoshima Y (1981) Studies of the phase transition in the single-lamellar liposomes. 2. liposome-size effect on the phase transition. *J Phys Chem* 85:1032–1037
- van Dijck PWM, Kaper AJ, Oonk HAJ, De Gier J (1977) Miscibility properties of binary phosphatidylcholine mixtures. *Biochim Biophys Acta* 470:58–69
- van Dijck PWM, de Kruijff B, Aarts PAMM, Verkleij AJ, de Gier J (1978) Phase transitions in phospholipid model membranes of different curvature. *Biochim Biophys Acta* 506:183–191
- van Meer G, Vaz LC (2005) Membrane curvature sorts lipids. *EMBO Rep* 6:418–419
- Veatch SL, Polozov V, Gawrisch K, Keller SL (2004) Liquid domains in vesicles investigated by NMR and fluorescence microscopy. *Biophys J* 86:2910–2922
- Yanagisawa M, Imai M, Masui T, Komura S, Ohta T (2007) Growth dynamics of domains in ternary fluid vesicles. *Biophys J* 92:115–125